Available online at www.sciencedirect.com
SCIENCE DIRECT®
Journal of Magnetic Resonance 161 (2003) 198–203
JMR Journal of Magnetic Resonance
www.elsevier.com/locate/jmr

Chemically selective NMR imaging of a 3-component (solid–solid–liquid) sedimenting system

Steven D. Beyea,[a] Stephen A. Altobelli,[a,*] and Lisa A. Mondy[b]

[a] New Mexico Resonance, 2301 Yale Blvd. SE, Suite C-1, Albuquerque, New Mexico 87106, USA
[b] Sandia National Laboratories Albuquerque, New Mexico 87185, USA

Received 9 September 2002; revised 12 November 2002

Abstract

A novel magnetic resonance imaging (MRI) technique which resolves the separate components of the evolving vertical concentration profiles of 3-component non-colloidal suspensions is described. This method exploits the sensitivity of MRI to chemical differences between the three phases to directly image the fluid phase and one of the solid phases, with the third phase obtained by subtraction. ^{19}F spin–echo imaging of a polytetrafluoroethylene (PTFE) oil was interlaced with ^{1}H SPRITE imaging of low-density polyethylene (LDPE) particles. The third phase was comprised of borosilicate glass spheres, which were not visible while imaging the PTFE or LDPE phases. The method is demonstrated by performing measurements on 2-phase materials containing only the floating (LDPE) particles, with the results contrasted to the experimental behaviour of the individual phases in the full 3-phase system. All experiments were performed using nearly monodisperse particles, with initial suspension volume fractions, ϕ_i, of 0.1.

Keywords: Sedimentation; Multi-phase; MRI; SPRITE

1. Introduction

Sedimentation/flotation of non-colloidal mixtures of particles and liquids has attracted scientific interest both because of its theoretical interest and its practical application to chemical and food processing. The primary focus of previous research into the physics of such systems has been in studies of two phase systems [1–4], in which a disperse solid particulate phase is settling in a continuous liquid phase. The rate of sedimentation depends upon the density difference of the solid and liquid phases, as well as the diameter and volume concentration of dispersed particles.

Numerous experimental studies have been performed on two-phase systems using a range of techniques, such as direct sampling, γ-ray tomography, optical transmission, and nuclear magnetic resonance imaging (MRI) [3–7]. These measurements provided experimental data on one-dimensional flow of the disperse particulates within the continuous liquid phase. Based on these studies, a variety of theoretical and empirical relations between volume fraction and hindered velocity have been developed [1,2,7]. These relations state that the presence of multiple particles results in a retardation of sedimentation velocity in a manner which depends upon local particle concentration, ϕ, i.e.,

$$v = v_0 G(\phi). \tag{1}$$

The coefficient G is the hindered settling factor, which has a value less than unity and relates the terminal velocity v_0 of an isolated particle to that of the clearing front, v, in a system containing many such interacting particles of the same size. While the above description has been given for sinking particles, the theory applies as well to rising particles [3].

The development of theoretical models for three-phase systems requires the determination of experimental data capable of providing spatial concentrations of individual phases at all stages of the clarifying process. However, three-phase systems, containing both a sinking and a floating solid phase, are difficult to study. This is because the above-mentioned experimental

* Corresponding author.
E-mail address: salto@nmr.org (S.A. Altobelli).

1090-7807/03/$ - see front matter © 2003 Elsevier Science (USA). All rights reserved.
doi:10.1016/S1090-7807(02)00172-6

methods are unable to discriminate different solid phases, during the period when the two solid phases are dispersed within each other.

NMR imaging methods have previously been used to study sedimentation/flotation processes by obtaining frequency encoded spin–echo images of the liquid phase, with the solid phase concentration obtained by subtraction [5–7]. While this is sufficient for determining spatial concentration of *total* solid content in a three-component mixture, it does not permit the discrimination of individual solid phases. We therefore describe a technique which utilizes the sensitivity of NMR to chemical differences in materials to discriminate NMR signals from individual phases.

2. Experimental setup

All NMR measurements were performed at 1.9 T in an Oxford horizontal bore superconducting magnet with a clear bore diameter of 310 mm, using a quadrature driven RF birdcage probe (Morris Instruments, Ottawa, ON, Canada) tuned to the ^{1}H frequency of 80.35 MHz, and a TecMag Libra spectrometer (TecMag, Houston, TX, USA). The gradient set (Magnex, Oxford, UK) had a maximum output of 4 G/cm, and was driven by Techron (Elkhart, IN, USA) 7700 amplifiers. Experiments were performed at an ambient temperature of approximately 21 °C.

3. Design of sedimentation/flotation phantoms

Selective discrimination of components by magnetic resonance requires the careful selection of materials used in the sedimentation phantoms. One common method of differentiating materials is to "null" a specific nuclear spin species, based upon differences in the spin–lattice relaxation time [8]. We have found, however, that quantitative imaging using this method requires a minimum delay of $5T_1$ to allow for complete recovery of the spin system, which places a limit on the RF pulse repetition time, and ultimately on the temporal resolution of the technique. We have therefore chosen to discriminate between the liquid and solid phases based upon nuclear spin species, and therefore resonant frequency.

Materials chosen for the sedimentation phantoms were therefore selected so two of the phases gave chemically distinct signals and the third phase none. Thus, a RF pulse applied at a specific frequency would lead to a detected NMR signal from only one of the three individual phases. We need only to obtain signals from two of the phases to determine the spatially resolved concentrations of all three components.

For a solid component we chose low-density polyethylene (LDPE). While many semi-crystalline hydrocarbon polymer plastics would be suitable (such as polyvinyl chloride (PVC) and acrylonitrile butadiene styrene (ABS)), LDPE has the advantage that it is fully hydrogenated and has a high amorphous content, which gives a strong NMR ^{1}H signal with a relatively narrow linewidth of approximately 2100 Hz. To differentiate liquid and solid signals we then chose a perfluorinated oil for the liquid phase. This oil contains no hydrogen while providing a strong ^{19}F NMR signal, and is available in a variety of viscosities. In our 1.9 T magnet, ^{1}H and ^{19}F resonant frequencies are 75.6 and 80.35 MHz, respectively.

The second solid phase was chosen to be spheres of borosilicate glass. This glass is negatively buoyant in perfluorinated oil, and has no significant NMR image intensity at either ^{1}H and ^{19}F frequencies. Therefore, an image acquired at a resonant frequency of 75.6 MHz will result in a spatial map of only the liquid concentration, while an image obtained at a resonant frequency of 80.35 MHz will produce a map of only the positively buoyant LDPE solid phase. While suitable candidates for NMR sensitive materials for all three phases can be found, imaging all three phases would only act to decrease the ultimate temporal resolution. However, using a third NMR sensitive material with a distinct Larmor frequency (such as ^{2}H or ^{29}Si) would permit studies of four-phase materials.

The sedimentation phantoms were made using LDPE grains (Ultra Chemical, Red Bank, NJ, USA) sieved to between 150 and 180 μm and glass spheres sieved to between 250 and 300 μm for the floating and sinking phases, respectively. These particular LDPE and glass spheres had a specific gravity of 0.919 and 2.5, respectively. All phantoms were produced using a viscous polytetrafluoroethylene (PTFE) Krytox GPL 105 oil (DuPont, Danbury, CT, USA) as the perfluorinated liquid phase. This oil has a specific gravity of 1.9, and a kinematic viscosity of 550 cST at 20 °C. Krytox has high purity, and we were unable to detect a ^{1}H signal from this oil. All phantoms were contained in acrylic right cylindrical vials with a 32-mm i.d. and a height of 34-mm. The particle sizes and oil viscosity were chosen so that sedimentation times were on the order of 1–2 h in this geometry.

To test the imaging method, both two-phase (containing only the buoyant LDPE solid phase) and three-phase (containing both the LDPE and glass solid phases) phantoms were created. The two-phase phantom consisted of a LDPE solid concentration (ϕ_{S1}) of 10% by volume, while the three-phase phantom consisted of a LDPE solid concentration of 10% and a glass solid concentration (ϕ_{S2}) of 10%.

The phantoms were slowly mixed for several minutes, with a thin rod, to ensure uniform dispersion of the solid particles without introducing air bubbles. Once the phantoms were mixed they were placed in the magnet

and NMR data acquisition typically commenced within 10 s.

4. NMR imaging method

The method used to image the sedimentation phantoms is to rapidly interleave sequences appropriate to imaging solids and liquids. Much like the choice of phantom materials themselves, this therefore requires a careful selection of NMR imaging pulse sequences that are ideally suited to imaging each individual phase.

The most technically challenging phase to image is the solid LDPE. Given that this material has a multi-component T_2 with a long component (corresponding to the amorphous phase) of 150 μs, most "conventional" imaging sequences are incapable of obtaining good S/N data. The SPRITE sequence [9] is a pure-phase encoding based method which has been used for imaging a variety of broadline materials, and is suitable for imaging of semi-rigid polymers such as LDPE [10,11].

The SPRITE method involves a series of broadband RF excitation pulses, applied in the presence of a gradient that is stepped through the full spectrum of phase encode values (see Fig. 1). Typical step lengths T_{step} are on the order of milliseconds. Given that the long T_1 component of LDPE is approximately 300 ms, RF pulses are applied at the Ernst angle [8]. In all current sedimentation experiments we used 64 k-space data points acquired with an 8 ms step delay (T_{step}), 360 μs phase encoding time (t_{enc}), a maximum phase encode gradient of 4 G/cm, and an Ernst angle excitation pulse of 2.5 μs ($a = 22°$). Fourier transformation of the data results in an image field-of-view of 5.5 cm. NMR spectrometer frequency was set to 80.35 MHz for excitation and detection.

Using the above imaging parameters, each k-space data line required 512 ms per scan. A cooling delay of 4.5 s was required between individual scans in order to prevent the gradient coils overheating, because the gradient set used in these experiments was not actively cooled. With the above acquisition parameters, the sedimentation phantoms required signal averaging 24 scans to obtain an image with good S/N, leading to a total imaging time per one-dimensional concentration profile of 120 s. The cooling delay therefore puts a lower limit on imaging speed, using our current equipment. The time per profile, however, is still much less than the time for sedimentation (1–2 h) using the phantoms described above.

The SPRITE gradient cooling delay is not totally wasted time, however, because a portion of this time is used to acquire the image data for the liquid phase. Following the end of the ^{1}H SPRITE acquisition, the spectrometer frequency is shifted to the ^{19}F resonance of 75.6 MHz, and a conventional spin–echo frequency-encoded pulse sequence is used to acquire an image of the PTFE liquid phase (see Fig. 1).

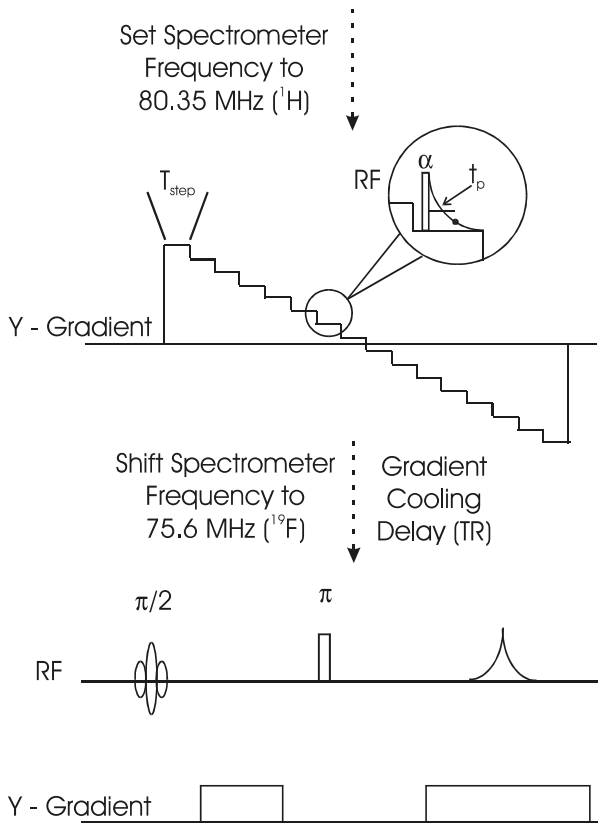

Fig. 1. NMR pulse sequence. SPRITE imaging of the LDPE solid phase is performed with RF excitation and detection at the ^{1}H frequency of 80.35 MHz. SPRITE is a pure phase encoding technique, which utilizes low flip angle RF pulses (α) applied during the presence of a magnetic field gradient, where t_p is the phase encoding time and T_{step} is the time between RF pulses. During the gradient cooling delay, required due to duty cycle restrictions, the spectrometer frequency is shifted to the ^{19}F frequency of 75.6 MHz. A conventional frequency encoded profile of the PTFE liquid phase is then performed, using a soft, chemically selective, excitation pulse to prevent chemical shift artifacts.

The ^{19}F excitation was a soft, chemical shift selective pulse, applied in the absence of a gradient. This is required because the NMR signal from the PTFE oil contains two groups of lines separated by a chemical shift of approximately 70 ppm. Therefore, imaging with a RF pulse which excites the entire ^{19}F spectrum of the oil leads to a severe chemical shift artifact. The selective RF pulse excites and encodes only one spectral grouping, thereby avoiding the image artifact.

All images of the PTFE liquid phase were acquired using a 5.4 ms echo time (TE), with 64 k-space data points acquired with a 1.4-G/cm read gradient and a 32-μs dwell time. The 180° pulse length was 300 μs at the ^{19}F frequency. Pulse repetition rate TR^{-1} was limited by the SPRITE gradient cooling delay. Therefore, 24 scans were averaged per one-dimensional profile with a TR of 5 s. The choice of read gradient strength and dwell time was made so that the ^{19}F liquid phase image exhibited the same field-of-view as the ^{1}H solid phase image.

Because the two resonance frequencies are only 4.7 MHz apart, our singly tuned RF probe is capable of exciting/detecting both resonances. In all experiments shown here, we used a RF probe with an unloaded Q-factor of approximately 150, tuned, and matched at the ^{1}H resonant frequency. We note that the although the ^{19}F resonance is significantly outside the bandwidth of the RF probe, we are able to sacrifice the majority of the PTFE signal because the signal from the oil is several orders of magnitude stronger (in a probe tuned to the ^{19}F frequency) than that from the LDPE solid. This results in NMR signals from the LDPE solid and the PTFE liquid which are comparable in amplitude.

5. Results and discussion

5.1. Two-phase experiments

We first applied the method to a two-phase system containing only the PTFE liquid and the LDPE buoyant solid phase. After placing the fully mixed phantom in the magnet, 60 one-dimensional vertical profiles of both phases were obtained over a 2-h period. The evolution of one-dimensional vertical concentration images for the PTFE liquid and LDPE solid phases are shown in Fig. 2a and b, respectively. Several representative one-dimensional plots are shown in Fig. 3.

The results clearly demonstrate the ability of this method to selectively resolve the individual spatial concentrations (ϕ) of the solid and liquid phases. Furthermore, the concentration images of the solid phase are shown to be equal to 100% minus the measured spatial concentration of the liquid phase, which validates that the method accurately measures the concentration of each phase simultaneously. The results show a sharp flotation clearing front which proceeds linearly with time, until the front approaches the compacted region. This behaviour is typical for two-phase sedimenting systems [3].

5.2. Three-phase experiments

The method was next applied to a three-phase system, containing both a floating LDPE solid phase and a sinking glass solid phase. Results were obtained using identical acquisition parameters as in the two-phase system, with 60 profiles of the solid LDPE and liquid PTFE phases obtained over a 2-h period.

Following Fourier transformation of the imaging data sets, the entire liquid phase data set was normalized so the mean value of liquid volume fraction ϕ_L in the clear fluid (fully settled) region was equal to 100%. Using this normalized data set, we calculated the mean ϕ_L in a region containing only LDPE solid and PTFE oil. The LDPE solid imaging data set was then normalized so the same region (containing only LDPE and PTFE oil) had a mean LDPE volume fraction ϕ_{S1} equal to 100% minus ϕ_L.

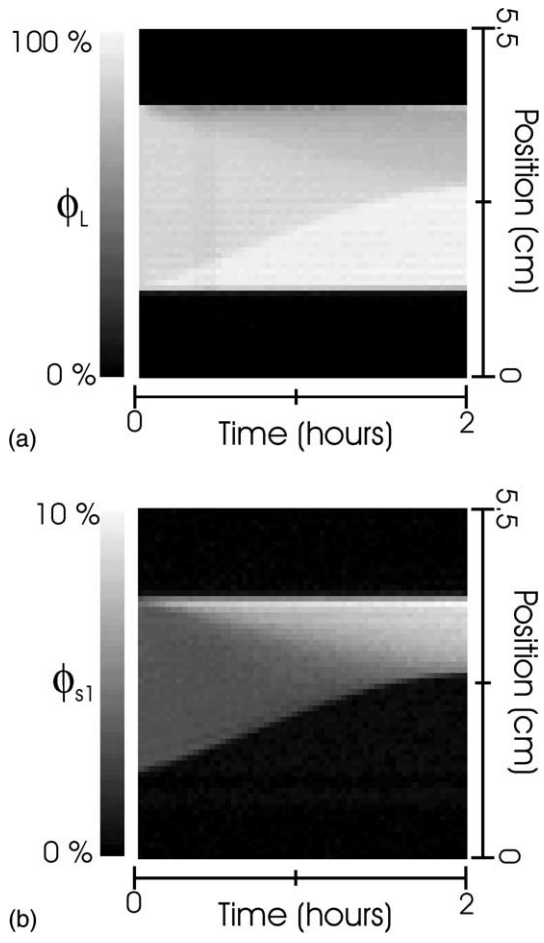

Fig. 2. One-dimensional images of volume fraction versus time for a 2-phase sedimenting system, shown for (a) PTFE liquid fraction (ϕ_L) and (b) LDPE solid fraction (ϕ_{S1}). Sixty profiles of each phase were acquired simultaneously over a 2 h period. Images are 64 points with a field-of-view of 5.5 cm.

The difference between the two normalized liquid and solid phase data sets leads to a spatial map of the volume fraction of the negatively buoyant glass solid phase ϕ_{S2}. Vertical concentration images versus time are shown for the PTFE liquid, LDPE solid, and glass solid phases in Fig. 4a–c, respectively. These results demonstrate the capability of the method to determine the spatial concentration of the NMR "invisible" solid phase, as the difference of the two experimentally measured phases.

Now we can compare behaviour of the two and three phase phantoms. The clearing front velocity of the LDPE solid in the three phase phantom is no longer constant in time. Indeed, during the period when the sinking and floating phases are dispersed within each other, the flotation velocity of the LDPE particles is higher than in the analogous two-phase phantom. Thus, the hindered flotation factor (Eq. (1)) has increased when the third phase was introduced and the floating and sinking particles are interspersed, even though the total local concentration of

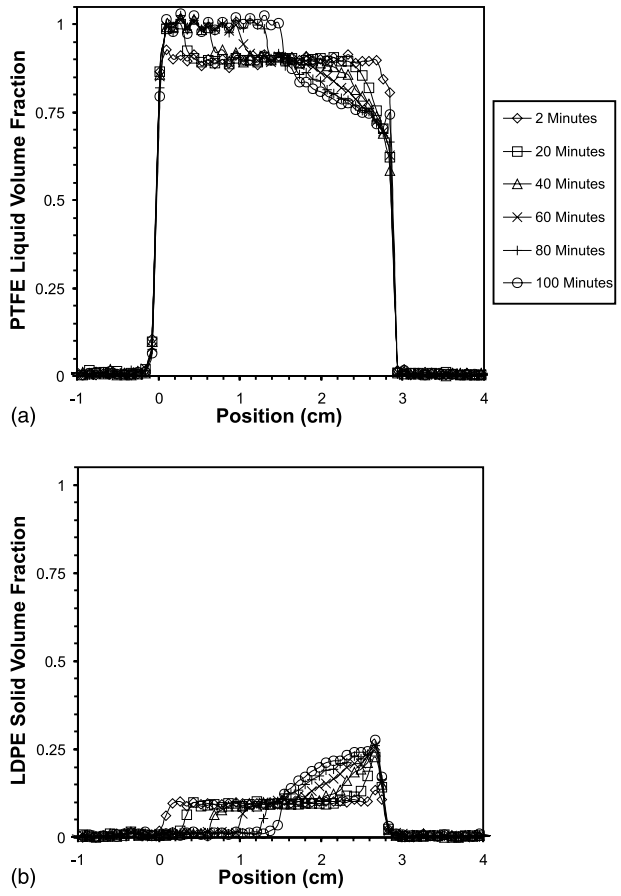

Fig. 3. Representative one-dimensional plots of (a) PTFE liquid fraction (ϕ_L) and (b) LDPE solid fraction (ϕ_{S1}), obtained from the data set shown in Fig. 2. Profiles are shown for evolution times of 2 (◇), 20 (□), 40 (△), 60 (×), 80 (+) and 100 (○) minutes after initial mixing.

particles is higher. This is evidenced by the higher initial flotation rate of the clearing front at early times in Fig. 4b ($\sim 5.7 \times 10^{-4}$ cm/s) relative to the clearing front in the analogous image in Fig. 2b ($\sim 2.9 \times 10^{-4}$ cm/s). Sedimentation/flotation velocity can be approximated by the instantaneous slope of the clearing front position versus time. Accurate determination of the hindered velocities in such systems, using more complex methodologies [7], will be the subject of future work.

The effect on sedimentation rates in multicomponent mixtures of particles with varying relative sizes has previously been noted in the literature [12–15]. However, only a limited amount of experimental data has been published on such systems. Future experiments will therefore systematically study the effect of varying relative velocities on the individual hindered sedimentation/flotation factors in three component systems.

6. Conclusions

We described a new experimental method that is capable of simultaneously resolving the one-dimensional spatial concentrations of the liquid and solid phases in a three-phase separating system. This method should provide information on the behaviour of multiphase sedimenting systems which cannot be provided by other methods.

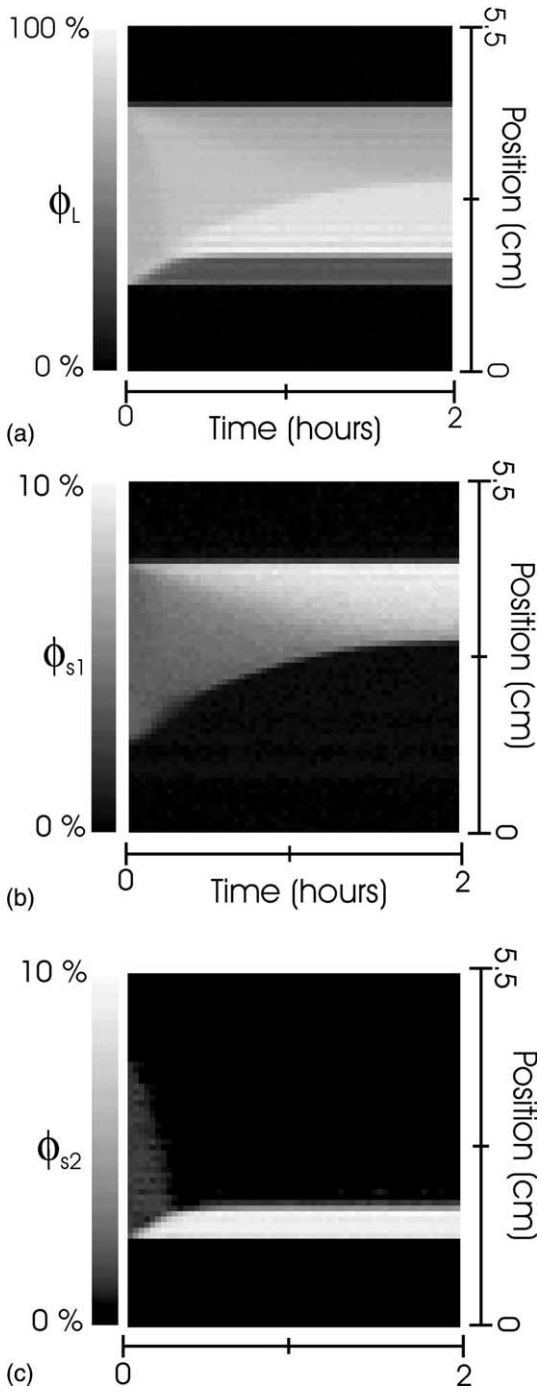

Fig. 4. One-dimensional images of volume fraction versus time for a 3-phase sedimenting system, shown for (a) PTFE liquid fraction (ϕ_L) and (b) LDPE solid fraction (ϕ_{S1}). Volume fractions of (c) the negatively buoyant glass phase (ϕ_{S2}) were obtained by subtraction with $\phi_{S2} = 100\% - [\phi_{S1} + \phi_L]$. Sixty profiles of each phase were acquired simultaneously over a 2 h period. Images are 64 points with a field-of-view of 5.5 cm.

The temporal resolution of the method is limited by maximum amplitude and duty cycle restrictions of the gradient coils. Water-cooled gradient coils, capable of providing 8 G/cm at 100% duty cycle will increase the temporal resolution to approximately 5 s per profile. The acquisition of concentration profiles with higher temporal resolution will permit accurate calculations of the functional relation between hindered velocity and volume fraction, called the "hindrance function" [7], for individual phases in multiphase systems. We are currently performing experiments to study how differences in the relative sedimentation velocity of individual solid phases affect the hindrance functions, in three phase systems compared to the corresponding two-phase systems.

Acknowledgments

The authors thank Ultra Chemical and Bruce P. Ulissi of DuPont for providing material samples, and Drs. Eiichi Fukushima and Dean Kuethe for useful discussions. S.D.B. and S.A.A. acknowledge the support of the US Department of Energy, Office of Basic Energy Sciences, Division of Materials Sciences and Engineering, via Grant No. DE-FG03-93ER14316. L.A.M. acknowledges the partial support of the Office of Basic Energy Sciences, Division of Chemical Sciences, Geosciences, and Biosciences, United States Department of Energy. Partial funding was also provided by a grant from the National Energy Technology Laboratory, United States Department of Energy. This work was supported by the US Department of Energy under Contract DE-AC04-94AL85000 at Sandia National Laboratories. Sandia is a multiprogram laboratory operated by Sandia, a Lockheed Martin, for the United States Department of Energy. These sponsorships do not constitute endorsements by the US Department of Energy of the views expressed in this article.

References

[1] J.F. Richardson, W.N. Zaki, Sedimentation and fluidization: Part I, Trans. Inst. Chem. Eng. 32 (1954) 35.
[2] G.J. Kynch, A theory of sedimentation, Trans. Faraday Soc. 48 (1952) 166.
[3] R.F. Probstein, Physicochemical Hydrodynamics, second ed., Wiley, New York, 1994 (Chapter 5).
[4] M.C. Roco (Ed.), Particulate Two-Phase Flow, Butterworth-Heinemann, Stoneham, MA, 1993.
[5] S. Lee, Y. Jang, C. Choi, T. Lee, Combined effect of sedimentation velocity fluctuation and self-sharpening on interface broadening, Phys. Fluids A 4 (1992) 2601.
[6] M.A. Turney, M.K. Cheung, M.J. McCarthy, R.L. Powell, Magnetic resonance imaging study of sedimenting suspensions of noncolloidal spheres, Phys. Fluids 7 (1995) 904.
[7] S.A. Altobelli, L. Mondy, Hindered flotation functions from NMR imaging, J. Rheol. 46 (2002) 1341.
[8] P.T. Callaghan, Principles of Nuclear Magnetic Resonance Microscopy, Clarendon Press, Oxford, 1991.
[9] B.J. Balcom, R.P. MacGregor, S.D. Beyea, D.P. Green, R.L. Armstrong, T.W. Bremner, Single-point ramped imaging with T_1 enhancement (SPRITE), J. Magn. Reson. A 123 (1996) 131.
[10] I.V. Mastikhin, B.J. Balcom, P.J. Prado, C.B. Kennedy, SPRITE MRI with prepared magnetization and centric k-space sampling, J. Magn. Res. 136 (1999) 159.
[11] C.B. Kennedy, B.J. Balcom, I.V. Mastikhin, Three dimensional magnetic resonance imaging of rigid polymeric materials using single-point ramped imaging with T_1-enhancement (SPRITE), Can. J. Chem. 76 (1998) 1753.
[12] R. Burger, F. Concha, K.-K. Fjelde, K.H. Karlsen, Numerical simulation of the settling of polydisperse suspensions of spheres, Powder Technol. 113 (2000) 30.
[13] R.H. Weiland, Y.P. Fessas, B.V. Ramarao, On instabilities arising during sedimentation of two-component mixtures of solids, J. Fluid Mech. 142 (1984) 383.
[14] R.L. Whitmore, The sedimentation of suspensions of spheres, Brit. J. Appl. Phys. 6 (1955) 239.
[15] Y.P. Fessas, R.H. Weiland, The settling of suspensions promoted by rigid buoyant particles, Int. J. Multiphase Flow 10 (1984) 485.